



HAL
open science

Influence of temperature and particle size on the single and mixed atmosphere gasification of biomass char with H₂O and CO₂

Chamseddine Guizani, Francisco Javier Escudero Sanz, Sylvain Salvador

► To cite this version:

Chamseddine Guizani, Francisco Javier Escudero Sanz, Sylvain Salvador. Influence of temperature and particle size on the single and mixed atmosphere gasification of biomass char with H₂O and CO₂. Fuel Processing Technology, 2015, 134, pp.175-188. 10.1016/j.fuproc.2015.01.031 . hal-01662704

HAL Id: hal-01662704

<https://hal.science/hal-01662704>

Submitted on 28 Feb 2018

HAL is a multi-disciplinary open access archive for the deposit and dissemination of scientific research documents, whether they are published or not. The documents may come from teaching and research institutions in France or abroad, or from public or private research centers.

L'archive ouverte pluridisciplinaire **HAL**, est destinée au dépôt et à la diffusion de documents scientifiques de niveau recherche, publiés ou non, émanant des établissements d'enseignement et de recherche français ou étrangers, des laboratoires publics ou privés.

Influence of temperature and particle size on the single and mixed atmosphere gasification of biomass char with H₂O and CO₂

C. Guizani *, F.J. Escudero Sanz *, S. Salvador

RAPSODEE, Mines Albi, Route de Teillet, 81013 Albi CT, Cedex 09, France

A B S T R A C T

The paper focuses on the gasification of biomass chars in H₂O, CO₂ and their mixtures. The first part is dedicated to the study of the influence of particle size and temperature in single atmosphere gasification experiments. The Thiele approach was successfully applied to assess the extent of diffusional limitations. We also studied the mixed atmosphere gasification of 0.2 mm chars at various temperatures and found that the char reactivity is fairly represented by an additive law at relatively low temperatures while it is lower than the sum of the individual contributions for high temperature cases. Similarly, we assessed the effect of particle size for mixed atmosphere experiments and found that an additive law was representative of the experimental reactivities for particle sizes from 0.2 to 13 mm. The present work provides useful and worthy information on the char gasification reactivity in conditions close to practical operating ones encountered in biomass gasifiers.

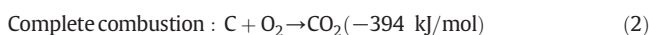
Keywords:

Biomass char
CO₂
H₂O
Reactivity
Mixed atmospheres
Thiele modulus

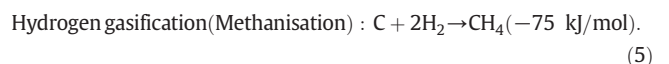
1. Introduction

Char gasification is an important step the global operation of biomass gasification. Indeed, when a biomass particle is gasified, it dries first, pyrolysis in second lieu, resulting in emission of gas species and formation of a solid char containing mainly carbon with some oxygen, hydrogen and mineral species in a far lesser amount. The produced char reacts with the gasification medium resulting in the production of additional gaseous species mainly composed by CO and H₂. The gasification reaction is the limiting step in the global gasification reaction and is of major importance in the sizing of gasifiers [1]. Inside a gasifier, the solid char can react with various gasifying agents such as O₂, H₂O, CO₂ and H₂. The gasifying agents have two origins: either they are provided by an external supply into the gasifier or are produced inside the gasifier by the drying and pyrolysis reactions. In most practical situations, the char reacts with a mixture of these species following the reaction of char combustion and gasification:

Char combustion



Char gasification



Huge literature exists on biomass char combustion and gasification with O₂, H₂O and CO₂. The reader can refer to Di Blasi's review on combustion and gasification rates of biomass chars [2]. A wide range of gasification kinetic data of various char biomasses is reported. On the contrary, few studies deal with the gasification of biomass char in complex atmospheres containing more than one gasifying agent in particular CO₂ + H₂O while it is of practical interest to study the effects of mixing the gases on the char gasification reaction, as it is representative of practical situation in gasifiers. For instance, inside a fixed bed gasifier, a char particle can be gasified simultaneously by more than a gasifying agent. It can also react at first with a gas "A", for instance CO₂, and then reacts with another one, a gas "B", H₂O for example, and vice versa. It's therefore of interest to study the mixed atmosphere gasification of chars as well as the mutual effects of gases on the char reactive properties, providing thus worthy information for near practical conditions encountered in such processes.

In mixed atmosphere gasification reactions, H₂O and CO₂ can react separately (*passive cooperation or additivity*), the reactivity in a mixed atmosphere of CO₂ and H₂O can be therefore expressed as the sum of

* Corresponding authors.

E-mail addresses: guizani.c@gmail.com (C. Guizani), javier.escuderosanz@mines-albi.fr (F.J. Escudero Sanz), sylvain.salvador@mines-albi.fr (S. Salvador).

the single reactivities. The two gases can also compete and react on shared active sites (*Competition*). The reactivity in mixed atmosphere of CO₂ and H₂O is therefore lower than the sum of the single reactivities. The third case, there can be synergy between the two gases (*synergy or active cooperation*) and the char reactivity in mixed atmosphere gasification experiments is higher than the sum of the single reactivities.

An overview on the literature focusing on complex atmosphere gasification of biomass chars shows for instance that Groeneveld and Van Swaaij [3] studied the wood char gasification reaction in a mixture of H₂O and CO₂. The authors proposed a *n*th order model for wood char gasification in a mixed atmosphere of H₂O and CO₂. The two reactions were assumed to have the same activation energy and the global reaction rate was dependant on the sum of the partial pressures of H₂O and CO₂.

Maria Barrio and co workers [4] performed experiments of wood char gasification in steam carbon dioxide mixtures. The authors found that the carbon conversion is mainly due to steam gasification mean while the carbon dioxide, which is less reactive, has potentially another role when it is injected as a co reactant with steam but in any case would inhibit the gasification reaction.

In 2008, Tagutchu et al. [5] observed a synergy between H₂O and CO₂ when mixed together as a gasifying agent. They found that the char reactivity in mixed atmospheres of CO₂ + H₂O was higher than the sum of the single reactivities and concluded to synergy effects between the two gases. They proposed a model based on the work of Robert and Harris [6] in which the H₂O and CO₂ react on separate active sites. As suggested in [5], the authors think that CO₂ creates additional micro porosity and enhances the access of H₂O to the active sites.

The gasification of a large variety of biomass samples was investigated in a TG apparatus with a heating rate of 10 °C/min up to 1000 °C using steam, carbon dioxide or a mixture of both reactants as a gasification medium [7]. The authors observed that regardless of the biomass type, introducing CO₂ with a minimum amount of 30% next to steam into the flow stream resulted in a complete char burnout with a light mineral film remaining in the crucible, whereas a black char residue remains when using only steam as a gasification medium. In a complementary study, the same authors reported several facts related to CO₂ addition as a co gasifying medium with steam such as the enhanced char micro porosity [8].

Susana Nilsson et al. studied the gasification of dried sewage sludge (DSS) chars in a pilot fluidized bed reactor under CO₂, H₂O and their mixtures [9]. The experiments were performed in a temperature range of 800–900 °C and a gas partial pressure of 0.1–0.3 bar. The authors demonstrated that the DSS char reactivity in mixed atmospheres of H₂O and CO₂ can be expressed as the sum of single atmosphere gasification reactivities.

Susana Nilsson et al. studied the gasification reactivity of olive tree pruning [10] in the same fluidized bed apparatus. The experiments were done in a temperature range of 760–900 °C in mixtures of CO₂, H₂O, H₂, CO and N₂. The authors determined the reaction kinetic constants respectively for the CO₂ and the H₂O gasification reactions. Afterwards, they performed gasification experiments in mixtures of H₂O and CO₂ and found that their experimental results are correctly described by summing the two single rates.

In our previous work on the gasification of HHR chars and LHR chars at 900 °C, we found that regardless of the pyrolysis conditions, and for various CO₂ + H₂O concentrations in the gasification medium, the char reactivity in mixed atmospheres can be fairly described by summing the single reactivities obtained respectively under H₂O and CO₂ [11].

The main results on biomass char gasification in mixed atmospheres of CO₂ and H₂O as discussed before are summarized in Table 1.

Studies on mixed atmosphere gasification of chars originating from coal or lignite are more numerous than those performed on biomass chars. It is of great interest to refer to them as the chars have several common features, but without forgetting that they are not identical to avoid hasty conclusions and non reliable comparisons. For instance, Lilledahl and Sjöström [12] studied the gasification of finely ground lignite char samples of 0.5–1 g in a thermo balance at atmospheric and elevated pressures, at temperatures between 750 and 850 °C, using a number of CO/CO₂/H₂O/Ar mixtures. The authors found that the mixed atmosphere char gasification reactivity can be modelled following a common active site reaction mechanism.

Roberts and Harris [6] performed a comparative study on the gasification of a charcoal in single atmospheres of H₂O and CO₂ and in a mixture of the two gases. In a mixed atmosphere, the char conversion rate decreased comparatively with that obtained in a pure steam gasification medium which led the authors to conclude the inhibiting effect of CO₂ on the steam gasification reaction. They proposed the model below assuming that there is a competition between steam and carbon dioxide for the same surface reaction sites. The authors made the assumption that the CO₂ carbon gasification reaction rate is so low that the reduction in the available surface area by adsorbed C(O) species from the CO₂ reaction is likely behind the decrease in steam gasification reaction upon addition of CO₂. These conclusions are nonetheless hasty as they were drawn for a 0–10% char conversion level. Carbon dioxide seems to inhibit the steam carbon reaction in the earlier stage of gasification, yet there is a lack of evidence to conclude the permanent inhibiting effect throughout the gasification reaction.

Everson et al. [13] also investigated the effect of a mixture of carbon dioxide and steam on the gasification of char coals. Firstly, they conduct gasification experiments in binary gas mixtures (H₂O + H₂ and CO₂ + CO) for the determination of the rate constants. The gasification reaction was best described with the assumption that the reactions occurred on separate sites.

More recently, Huang et al. [14] carried the same gasification experiments as Everson et al. They determined the different gasification constants by studying the char gasification with the binary gas mixtures H₂O + H₂ and CO₂ + CO. Experiments with multi component gasifying mixtures (H₂O + H₂ + CO₂ + CO) were also carried out showing results that fit well with the “separate reactive sites” reaction model given above. The comparison was based on the char reactivity at a conversion level of 50%. The calculated predictions according to the model were very close to the experimental values.

The assumption of reaction on separate active sites was also held by Tay et al. [15] for coal char gasification. The authors performed gasification experiments at 800 °C with different gasification atmospheres (15%

Table 1
Literature review on biomass char gasification in mixed atmospheres of CO₂ and H₂O.

Reference	Char	Pyrolysis conditions	Mixed atmosphere mechanism
[3]	Wood char (4 cm)		Same activation energy and dependance on the sum of partial pressure
[4]	Birch wood char (45–63 μm)	Slow pyrolysis 24 °C/min	Competition
[5]	Pine wood char (5.5 mm)	Medium rate pyrolysis in a screw reactor at 60 °C/s	Synergy
[7]	Various biomasses	Slow pyrolysis 10 °C/min	Synergy
[9]	Dried sewage sludge char (1.2 mm)	Fast pyrolysis in FBR	Additivity
[10]	Olive tree pruning char (1.9 mm)	Fast pyrolysis in FBR	Additivity
[11]	Beech wood char (1 mm)	Fast pyrolysis 100 °C/s Slow pyrolysis 5 °C/min	Additivity

H₂O balanced with Ar; 4000 ppm O₂ balanced with CO₂; 4000 ppm O₂, 15% H₂O balanced with CO₂) and gasification holding times. Char conversion rate calculations show that the degree of char conversion during the gasification in an O₂ + H₂O + CO₂ mixture was approximately equal to the sum of those during the gasification in 15% H₂O (balanced with argon) and in O₂ + CO₂ mixture. They suggest that the additivity in char conversion means that O₂, H₂O and CO₂ do not compete for the same active sites on the coal/char.

More recently, Chen et al. [16] investigated the effect of the pyrolysis conditions on the gasification reactivity of lignite chars in mixtures of H₂O + CO₂. Two kinds of char were prepared from a lignite by fast pyrolysis using a drop tube furnace and by slow pyrolysis using a fixed bed furnace at a temperature of 1273 K. Char gasification reactions with CO₂, H₂O and their mixtures were performed in a thermogravimetric analyser (TGA) system. The gasification rate equations derived from TGA were afterwards validated by fluidized bed gasification experiments. The authors found that both fast chars and slow chars were dense. The shrinking core model was able to predict gasification of both fast char and slow char, which means that the reaction occurs mainly in the external surface. The authors found that the char gasification rate in the mixtures of CO₂ and H₂O was lower than the sum of the two single reaction rates, but higher than the rate of each independent reaction, for both fast char and slow char gasification. The gasification rate in a mixture of H₂O and CO₂ was linearly dependant on the CO₂ single gasification rate. The gasification rate in mixtures of both gases could be written as a linear combination of the two single gasification rates. The regressed coefficient of R_(CO₂) is about 0.65 and the coefficient of R_(H₂O) is about 1 for both fast char gasification and slow char gasification. Both of the results from the TGA and the fluidized bed reactor showed that the char H₂O reaction was independent of char CO₂ reaction, while the char CO₂ reaction was inhibited by the char H₂O reaction.

Umemoto et al. [17] studied the coal gasification reaction in mixed atmospheres of CO₂ and H₂O. The coal chars were prepared in a drop tube furnace at 1673 K. The authors performed gasification reaction in a TG apparatus. They found that the gasification reaction rate in mixed atmospheres was neither well described by a model where the H₂O and CO₂ react on separate active sites (the model over predicted the experimental data), nor by a common active site model as it under predicted the gasification rate. The authors proposed that the two reactants, H₂O and CO₂, partially share their respective active sites. The authors modified the LH expression for the chemical reaction rate term proposed by Everson et al. and introduced new parameters to account for the sharing of the active sites. The authors found that the greater contribution to the char gasification was from the steam gasification reaction. They think that this fact is due to the lower molecular size of the H₂O molecule which can penetrate in all the pores.

Bai et al. [18] recently studied the coal char gasification reactivity with CO₂ and H₂O and their mixtures. The coal samples were pyrolyzed under an argon atmosphere at temperatures of 800 °C, 900 °C, 1000 °C and 1100 °C adopting slow pyrolysis operating conditions, then gasified isothermally in CO₂ and H₂O environments ranging from pure CO₂ to pure H₂O in 20 vol.% increments. The authors found that at temperatures of 900 °C, 1000 °C and 1100 °C, the coal char has a maximum reactivity in a 100% H₂O atmosphere. Its reactivity decreases with CO₂ addition. However, at a temperature of 800 °C, the coal char has a higher reactivity in a mixed atmosphere than in pure H₂O or pure CO₂. Even more, the reactivity in a mixed atmosphere of CO₂ and H₂O was higher than the individual reactivities in H₂O and CO₂ respectively. The same results were obtained at 750 °C. The mixed atmosphere gasification showed competition beyond 800 °C and synergy at 800 °C and below [18]. These differences were found to be linked to catalytic effects due to calcium species.

The main results on coal and lignite char gasification in complex atmospheres are summarized in Table 2.

As reported in Tables 1 and 2, mixed atmosphere gasification reactions were tested for various biomasses and coal chars with various

Table 2
Literature review lignite and coal char gasification in complex atmospheres.

References	Fuel type	Pyrolysis	Mixed atmosphere mechanism
[12]	Lignite char (200–900 μm)	Slow pyrolysis	Competition
[6]	Coal char (600 μm)	Slow pyrolysis 10 °C/min	Competition
[13]	Coal char (20–70 μm)	Slow pyrolysis 20 °C/min	Additivity
[14]	Coal char (20 μm)	Fast pyrolysis in FBR 1000 °C/s at 840 °C	Additivity
[15]	Coal char (63–150 μm)	Fast pyrolysis in FBR at 800 °C	Additivity
[16]	Lignite char (70–106 μm)	Slow pyrolysis 10 °C/min Fast pyrolysis in FBR at 800 °C	Competition
[17]	Coal char (40 μm)	Fast pyrolysis in DTF at 1400 °C	Competition
[18]	Coal char (125 μm)	Slow pyrolysis 10 °C/min	Synergy below 800 °C and inhibition beyond

particle sizes going from several tenths of millimeter to several millimeters. The char preparation conditions as well as the gasification temperature and gas pressure were different from one study to another. The mechanisms proposed for the mixed atmosphere gasification also differ from one study to another. These observations mean that the validity of a mechanism (additivity, competition or synergy) depends on the experimental conditions as well as on the nature of the char.

One ambiguous issue that is still not well clarified is the issue of intrinsic conditions. In fact, the size of a char particle and the reaction temperature are determining factors in whether the gasification rate is controlled by the rate of chemical reactions, heat and mass transfer or both. It is acknowledged that the smaller the particle the more uniform the gas concentration and temperature inside it. In the case of concentration and temperature uniformity inside the char particle, gasification would be chemically controlled and heat and mass transfer limitations would not influence the reaction rate. Increasing the char particle size introduces heat and mass transfer limitations, until it reaches a critical size above which heat and mass transfer limitations predominate. In several studies [19,20], the authors pointed out that biomass apparent reactivity decreases when increasing the particle size, which is due to an increasing diffusional resistance.

Many authors propose a maximal particle size below which the gasification rate is constant and is consequently performed in the chemical regime, however the values are quite disparate from one study to another. For instance, Mermoud et al. proposed 1 mm as a critical size below which char steam gasification is chemically controlled at 900 °C [21]. Van De Steene et al. [22] found that the particle thickness was the characteristic dimension for parallelepiped shaped pine char. They also found that for particle thickness below 2.5 mm, the char steam gasification is chemically controlled at 900 °C. Gomez Barea et al. [19] found that the CO₂ gasification reaction of char from pressed oil stone is chemically controlled for powder char particles of 0.06 mm, in a temperature range of 800 to 950 °C which is quite different from the values given above. Klose et al. proposed that H₂O char and CO₂ char gasification reactions are performed in the intrinsic regime for particle sizes below 0.125 mm in a temperature range of 750 to 780 °C and 10 mg of sample mass. Isothermal gasification experiments were done in a thermogravimetric apparatus [23].

This variety of statement about intrinsic conditions shows well that it is quite difficult to state the nature of the gasification regime with assurance. It depends highly on the experimental conditions as well as on the texture of char. This issue will be discussed in the frame of the present work. The first aim of the present work is to provide data on char reactivity to H₂O and CO₂ and their mixture in practical gasification operating conditions. We also aim to evaluate the extent of diffusional limitations when varying the temperature and particle size. The aim is

Table 3
Proximate and ultimate analyses of the beech wood-chips (% dry basis).

Proximate analysis			Ultimate analysis			
VM	Ash	FC	C	H	O	N
88.1	0.4	11.5	46.1	5.5	47.9	0.1

also to shed light on the influence of temperature and char particle size on the multi component gasification reaction with CO₂ and H₂O.

2. Material methods

2.1. Low heating rate char preparation

The raw biomass samples are beech wood spheres with a 20 mm diameter. Proximate and ultimate analyses of the wood samples are given in Table 3. Low heating rate chars were prepared by a slow pyrolysis of the wood spheres under nitrogen. The pyrolysis was performed in a batch reactor. The wood spheres were placed in a metallic plateau, and spaced enough to avoid chemical and thermal interactions. The plateau was introduced into the furnace heated zone which was progressively heated under nitrogen from room temperature to 900 °C at 5 °C/min. The chars were kept for 1 h at the final temperature, cooled under nitrogen and stored afterwards in a sealed container. The low heating rate is expected to ensure good temperature uniformity in the wood particle and to lead to a quite homogeneous wood char, from the structural and chemical viewpoints, as demonstrated by [24] and pointed out by [25] and [26]. During the pyrolysis reaction, the char particles shrink and get an ovoid form. The mean particle diameter, calculated as the average of the three particle dimensions was estimated at 13 mm.

Some of the 13 mm char particles were afterwards ground with a mortar and a pillar. Several particle size fractions, on a wide particle size ranging from 0.04 mm to 13 mm, were retained for gasification experiments: char particles of 0.04 mm (char004), 0.2 mm (char02), 0.35 mm (char035) and 1 mm (char1) screen size, and finally the 13 mm (char13) char particles. The wood and char samples are shown in Fig. 1.

To ensure the chemical and structural homogeneity inside the 13 mm char particle, the char structure and chemical composition were analysed at three locations: at the surface, at half the distance from the centre and at the centre. Elemental composition and Raman spectroscopy were used to check particle homogeneity. The Raman spectra of the chars were recorded with a WITec Confocal Raman Microscope (WITec alpha300 R, Ulm, Germany) equipped with a Nd:YAG excitation laser at 532 nm. Table 4 shows the mean elemental composition of the char sample at the three locations (surface, half distance from the core and particle core). The standard deviations are quite low showing chemical composition homogeneity throughout the char particle.

Normalized Raman spectra with respect to the G peak height are shown in Fig. 2a. The normalized Raman signals are identical at the three locations attesting to the structural homogeneity of the char particles. The Raman spectra show in the first order region (800–2000 cm⁻¹), two main broad and overlapping peaks with maximum intensities at 1350 cm⁻¹ and 1590 cm⁻¹ [27]. In the literature, we frequently refer to these two peaks as respectively the D and G bands.

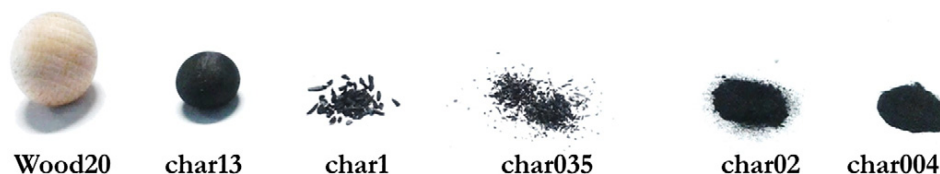


Fig. 1. Initial beech wood (left) sphere and derived char samples (decreasing size from left to right).

Table 4
Ultimate analysis of the wood-char samples.

C (wt.%)	H (wt.%)	O (wt.%) (by difference)	N (wt.%)	Ash (wt.%)
90.83 ± 0.93	0.676 ± 0.07	7.03	0.21 ± 0.027	1.25 ± 0.13

Deconvolution of the Raman signal into five bands corresponding to five carbon structures composing the char shows that the prepared char contains an amorphous phase (D3 band). The D3 band area decreases as the carbon gets ordered at higher temperatures. The D3 band is typical of disordered carbonaceous materials like coke, coal and biomass chars. These results are in accordance with those of [24] who evidenced the large char particle homogeneity when prepared in low heating rate conditions.

2.2. Char gasification experiments in H₂O, CO₂ and their mixture

2.2.1. The Macro TG experimental device and procedure

The M TG device is described in detail in our previous work on char gasification in mixed atmospheres of CO₂ and H₂O [11]. In general terms, the experimental apparatus consists of a 2 m long, 75 mm i.d. alumina reactor that is electrically heated, and a weighing system comprising an electronic scale having an accuracy of ±0.1 mg, a metallic stand placed over a scale on which a 1 m long, 2.4 mm external diameter hollow ceramic tubes are fixed. The ceramic tube holds the platinum basket in which the biomass particles are placed. The gas flow rates are controlled by means of mass flow meters/controllers. The gas flow inside the reactor is laminar and flowing at an average velocity of 0.20 m/s.

2.2.1.1. Gasification of char004 and char02. Char004 and char02 are in the form of powders. A char mass of 100 to 130 mg is spread out on the whole surface of the 50 mm diameter platinum basket in the form of a very thin layer. The char mass may seem important compared to what is introduced in classical TG devices but the surface of the crucible is large enough (0.002 m²) to allow spreading this mass in the form of a thin layer. The char is directly exposed to the surrounding atmosphere as the platinum basket is simply in the form of a circular plane without any side wall.

2.2.1.2. Gasification of char035, char1 and char13. Char035 and those of greater sizes can be distinguished and placed individually. The char particles are spread over the platinum basket and spaced enough to avoid thermal and chemical interaction. For the char samples char035 and char1, about 20 to 40 particles are spread on the platinum basket. For the char13 samples, 2 particles are placed on the platinum support for a total mass of nearly 1.2 g.

2.2.1.3. The gasification procedure. The platinum basket bearing the char particles and the ceramic tube holding it are first at room temperature. They are introduced in the hot reactor zone (which is at the gasification temperature) within less than 20 s, under a flow of nitrogen. The system has to get stabilized thermally as well as mechanically (due to the force of the flowing nitrogen over the basket) so that the mass displayed by the electronic scale becomes constant. This can be achieved within 5 min as depicted in Fig. 3.

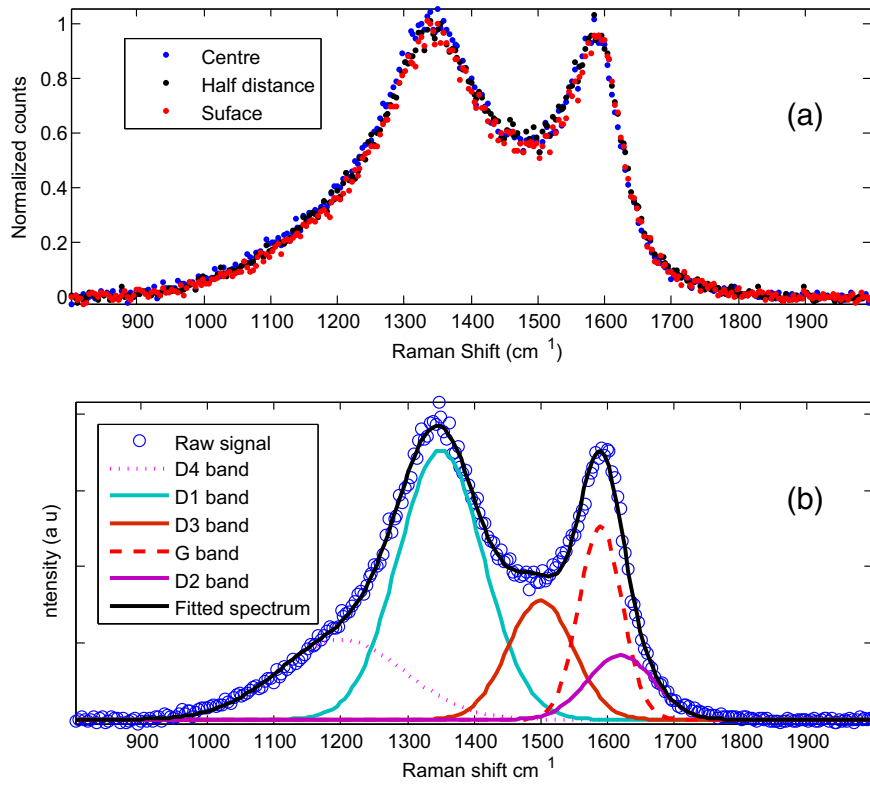


Fig. 2. Normalized Raman spectra (a) of the parent char at three locations of the particle (surface, half distance from the core and particle core) and spectrum deconvolution (b).

Afterwards, the gasification medium is introduced. The char gasification experiments were performed with CO_2 and H_2O and their mixtures. The MTG system allows recording char mass at frequencies from 0.1 s to 10 s. In the present work, the char mass was recorded per second. The data are afterwards smoothed so that we can reduce the noise in the derivative curves of gasification rate and reactivity.

2.2.2. Operating conditions

The operating conditions in terms of temperature and atmosphere composition for the different char gasification reactions including single

atmosphere gasification reactions, mixed atmosphere gasification and gas alternation experiments are listed in Table 5.

2.2.3. Theoretical modelling of the single atmosphere gasification reactions

The char apparent reactivity towards a gas can be expressed as in the following:

$$R(X)^{app} = \frac{1}{1-X(t)} \times \frac{dX(t)}{dt} \quad (6)$$

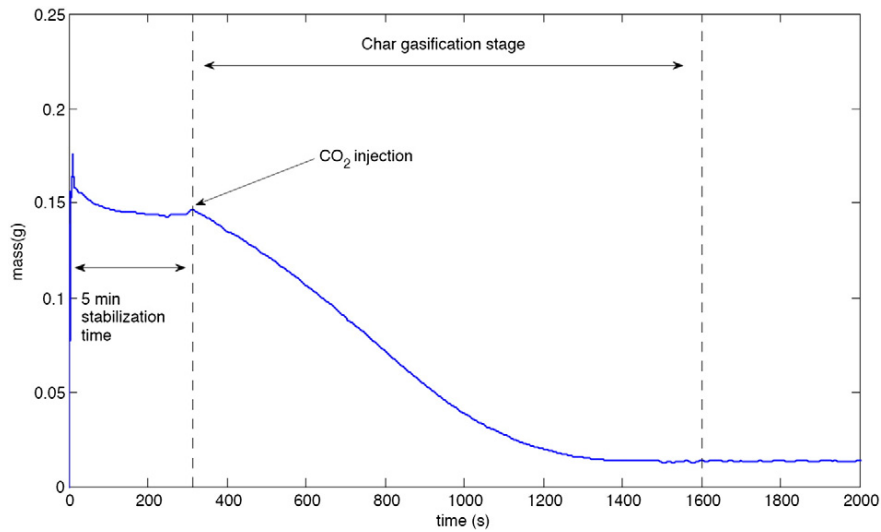


Fig. 3. Illustration of the gasification procedure (the case of CO_2 gasification).

Table 5
Char gasification experiments.

Samples	CO ₂ gasification	H ₂ O gasification	Mixed atmospheres
Char004	900 °C	900 °C	–
	0.2 atm	0.2 atm	–
Char02	850–900–950	800–850–900	900 °C
	1000–1100 °C	1000–1100 °C	0.2 + 0.2 atm
Char035	900 °C	900 °C	–
	0.2 atm	0.2 atm	–
Char1	900 °C	900 °C	–
	0.2 atm	0.2 atm	–
Char13	900 °C	900 °C	900 °C
	0.2 atm	0.2 atm	0.2 + 0.2 atm

where X is the conversion level given by:

$$X_{(t)} = \frac{m_0 - m_{(t)}}{m_0 - m_{ash}} \quad (7)$$

where m_0 , m_t and m_{ash} are respectively the initial mass of char, the mass at time t and the mass of the residual ash. If the gasification reaction is performed in the chemical regime (relatively low temperature and small particle size), the calculated reactivity would be the intrinsic one. As stated above, char reactivity depends on the operating conditions (temperature and reactant gas pressure), and char properties (texture, mineral content, structure). It is thus commonly expressed as the product of reference reactivity $R(X_{ref})_{(T,P_i)}$ (depending on the temperature and reactant gas pressure) and a structural term $f(X)$ accounting for the char property evolution along the conversion. Owing to the difficulties in the monitoring of the intrinsic char properties along the conversion, the structural term is usually an empirical correlation where the conversion level appears as the sole variable. Changes in the char intrinsic properties are implicitly described by this empirical term. The reference reactivity corresponds to a specific conversion level. Reference reactivity at 10% or 50% of conversion has been used in the literature [19,28,29]. The reactivity at the 50% conversion level ($R(50)$) is most

frequently used as a reference value. The reactivity at any gasification stage can be thus expressed as:

$$R(X)_{(T,P_i)}^{int} = R(50)_{(T,P_i)}^{int} f(X) \quad (8)$$

where $R(50)_{(T,P_i)}^{int}$ is the intrinsic reactivity at $X = 50\%$ and $f(X)$ is the structural function expression describing the evolution of the char properties during the gasification.

n th order kinetics are often used to express the temperature and CO₂ pressure dependence of $R(50)_{(T,P_i)}^{int}$. By assuming Arrhenius type kinetics for the kinetic constant, the intrinsic reactivity can have the following expression:

$$R(50)_{(T,P_i)}^{int} = M_C S_r k_{(T)} P_g^n \quad (9)$$

where M_C is the carbon molecular weight, S_r is the reactive surface ($m^2 \cdot kg^{-1}$), $k_{(T)}$ the kinetic rate constant of char gasification ($mol \cdot s^{-1} \cdot m^2 \cdot atm^{-n}$) and P_g is the reacting gas partial pressure at the particle surface (atm).

$k_{(T)}$ is expressed following an Arrhenius type law:

$$k_{(T)} = A \exp \frac{-E}{RT} \quad (10)$$

where A is the pre exponential factor ($mol \cdot s^{-1} \cdot m^2 \cdot atm^{-n}$), E is the char gasification activation energy (J/mol), R is the universal gas constant (J/(mol·K)) and T is the temperature (K).

For macroscopic char particles, there exist diffusional limitations [19]. One can no longer speak about a volumetric reaction rate (intrinsic) as the gas concentration inside the particle is not uniform. In this kind of situation there is a competition between gas diffusion and reaction inside the char particle. To model such a situation, one must solve the gas mass and energy conservation equations along the reaction to obtain the gas concentration profiles at any time and any location in the particle [20]. Although it is rigorous, numerical modelling requires too high computing capacities. There exist alternative methods for

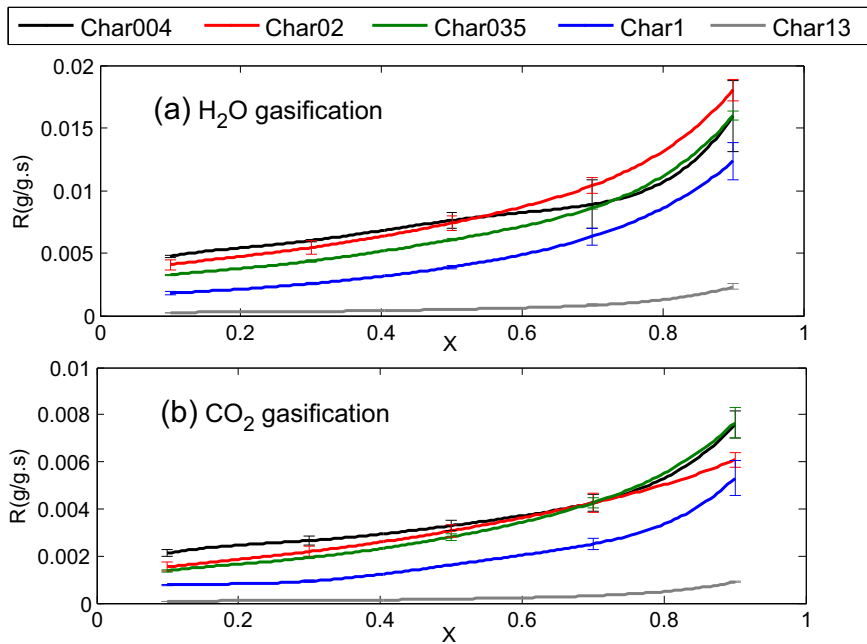


Fig. 4. Influence of particle size on the char gasification reactivity at 900 °C with 20% H₂O (a) and with 20% CO₂ (b).

formulating the apparent gasification reaction rate. The simplest method is using the pseudo activation energy which changes with temperature. However, this method cannot express the effect of the particle size and is poorly describing the physical phenomena. The evolution of the gasification rate with particle size can be described through a semi empirical expression, where the apparent reaction rate is expressed as a function of the intrinsic reaction rate and the particle size [30]. The third method consists of the effectiveness factor approach to take into account the diffusion reaction competition [31–34]. We will use this method in the present work to account for diffusional limitations when varying the char particle size or temperature.

The effectiveness factor approach originates from the catalyst theory. In the presence of diffusion reaction competition, Thiele [35] defined an effectiveness factor η which is the ratio of the apparent reaction rate to the intrinsic one. It allows taking into account the consumption of the reactant gas while it diffuses inside the porous particle. It is equal to unity in the absence of diffusional limitations and tends towards zero in the presence of high diffusional limitations. Using the effectiveness factor, the apparent reactivity reads:

$$R(50)_{(T,P_i)}^{app} = \eta R(50)_{(T,P_i)}^{int} \quad (11)$$

with η being the Thiele effectiveness factor.

The reaction order of biomass char gasification differs from one study to another. In Di Blasi's review, CO₂ char gasification reaction order varies between 0.36 and 1.2 and that of H₂O char gasification is comprised between 0.4 and 1 [2]. When using the effectiveness factor approach to model the effect of LHR char gasification, we will consider the gasification reactions as first order reactions. The definition of the effectiveness factor is rigorous only for a first order reaction. The effectiveness factor expression is obtained by volume integration of the reactant gas balance equation and has the following expression for spherical particles:

$$\eta = \frac{3}{\phi} \left(\frac{1}{\tan h\phi} - \frac{1}{\phi} \right). \quad (12)$$

The Thiele modulus ϕ has the following expression:

$$\phi = \frac{d_{part}}{2} \sqrt{\frac{\beta S_v k(T) P_g}{M_g D_{i,eff} C_g}} \quad (13)$$

where d_{part} is the particle diameter (m), β is a stoichiometric coefficient equal to the ratio between the gas molar mass and that of carbon, S_v is a volumetric surface (m²/m³), M_g is the molecular weight of the reactant gas (kg·mol⁻¹), C_g is the bulk concentration of the reactant gas (mol·m⁻³) and $D_{i,eff}$ is the effective diffusion coefficient (m²/s).

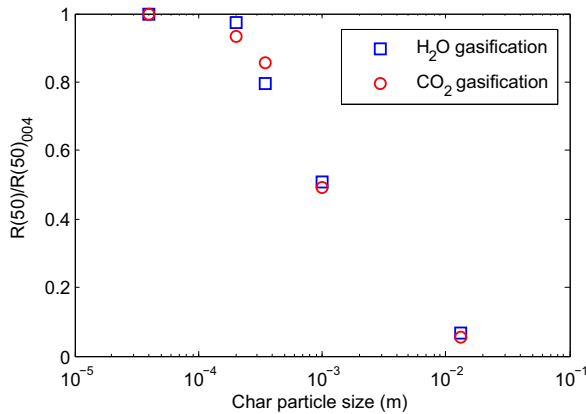


Fig. 5. Normalized R(50) with respect to that of char004 for H₂O and CO₂ gasification.

For a gas “i” (CO₂ or H₂O), $D_{i,eff}$ is expressed through the molecular diffusion coefficient $D_{i,mol}$ and the Knudsen diffusion coefficient $D_{i,Knudsen}$:

$$D_{i,eff} = \frac{1}{\frac{1}{D_{Knudsen}} + \frac{1}{D_{i,mol}}} \quad (14)$$

$$D_{i,mol} = a_i 10^{-5} \left(\frac{T}{298} \right)^{1.75} \quad (15)$$

$$D_{i,Knudsen} = \frac{\varepsilon}{\tau} 0.97 \frac{d_{pore}}{2} \left(\frac{T}{M_i} \right)^{0.5} \quad (16)$$

where a_i is a constant taken to be 1.67 for CO₂ and 2.1 for H₂O [33], d_{pore} is the pore diameter (m), ε is the char porosity and τ is the char tortuosity.

Several authors used the effectiveness factor approach to model the char combustion and gasification reaction for different temperatures and particle sizes [19,31,33–34,36–38]. The effectiveness approach renders the calculation of the char reactivity straightforward. Despite it not gathering all the physics of the gasification reaction, it is a simple method allowing the prediction of the char apparent reactivity without enormous computational effort.

2.2.3.1. Modelling procedure. At 50% of conversion we adopted a char porosity of 0.95, a tortuosity of 3 and an apparent density of 250 (kg/m³) (the initial density after pyrolysis is around 500 (kg/m³)). We measured the Total Surface Area of char02 at X = 0.5 by N₂ adsorption at 77 K. The values were 1230 (m²/g) for H₂O gasification and 840 (m²/g) for the CO₂ gasification. We used these values for the parameter S_v as well as in the calculation of S_v which is the product of S_r by the apparent density.

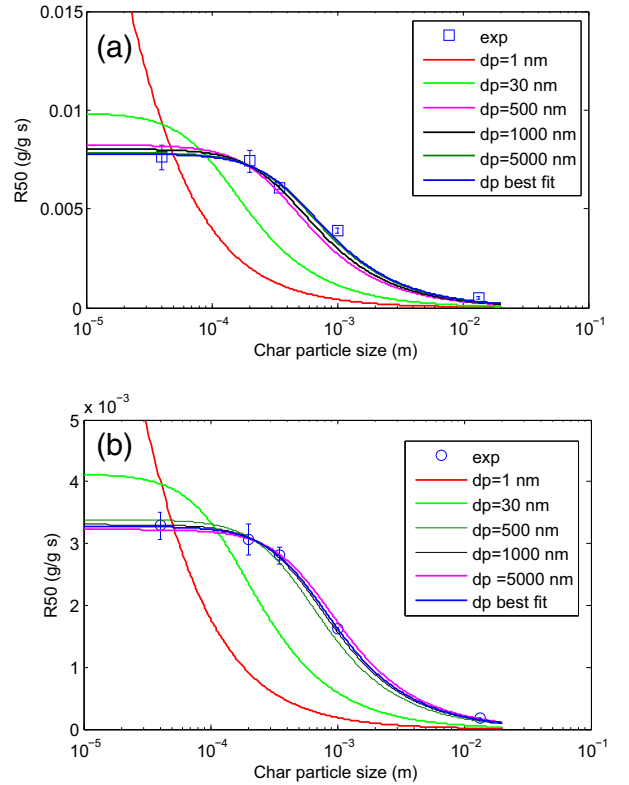


Fig. 6. Experimental R(50) and Thiele model for H₂O (a) and CO₂ (b) char gasification at 900 °C.

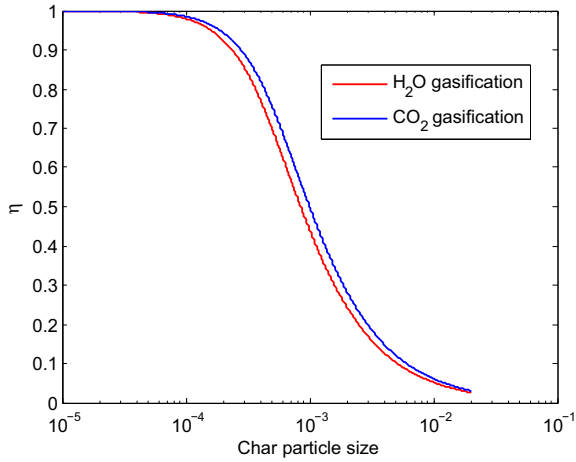


Fig. 7. Evolution of the effectiveness factor with the char particle size for H₂O and CO₂ gasification at 900 °C.

In the Thiele modulus expression, there are three unknown parameters that will be determined by best fitting the model to the experimental data. These parameters are d_{pore} in the effective diffusivity expression, A and E in the rate constant expression. d_{pore} and k_{900} are determined first by fitting the experimental R(50) data obtained at 900 °C for char004, char02, char035, char1 and char13 with the model. A and E are afterwards determined by best fitting the experimental R(50) data obtained for the char02 at different temperatures: 800 °C, 850 °C, and 900 °C for H₂O gasification, and 850 °C, 900 °C, 950 °C and 1000 °C for CO₂ gasification.

d_{pore} , A and E are determined by the minimisation of the following objective function:

$$OF = \sum_{j=1}^n \left(R(50)_j^{model} - R(50)_j^{exp} \right)^2. \quad (17)$$

2.2.4. Mixed atmosphere gasification reaction modelling

In the present work, we propose to model the mixed atmosphere reactivity as a linear combination of the single reactivities with CO₂ and H₂O following:

$$R(mix) = \alpha R_{(H_2O)} + \beta R_{(CO_2)}. \quad (18)$$

In the case of passive cooperation, the char reactivity in the mixed atmosphere is equal to the sum of the individual reactivities, and α and β would be both equal to 1. In the case where the two gases compete for the same active sites, the global reactivity is lower than the sum of the individual ones. α and β would vary between 0 and 1 without both reaching unity (in the case of passive cooperation). If α or β equals zero, only one gas is operating while the other is a spectator. Intermediate values depict the contribution of the gases to the global reaction. If there is a synergy, the global reactivity is higher than the sum of the individual ones. One or both coefficients will be higher than 1.

In the present work, we study the variation of these coefficients with the temperatures (800 °C, 900 °C, 1000 °C and 1100 °C) for the 0.2 mm size particles, as well as the variation with the char particle sizes considering the char02, char5 and char13 sample gasification at 900 °C.

α and β are determined by the minimisation of the following objective function:

$$OF = \sum_{j=1}^n \left(R(mix)_j^{model} - R(mix)_j^{exp} \right)^2. \quad (19)$$

This approach assumes that the contributions of the H₂O and CO₂ gasification reactions are constant along the reaction.

3. Results and discussion

3.1. Effects of particle size on char gasification reactivity in single atmospheres of H₂O and CO₂

Fig. 4 shows the influence of particle size on the char gasification reactivity towards H₂O (a) and CO₂ (b) gasification. It can be clearly seen that the char reactivity decreases when increasing the particle size due to increasing diffusional limitations. Char02 reactivities are quite close to that of char004 for both H₂O and CO₂ gasification. This means that at 900 °C and for these particle sizes the gasification conditions approach the intrinsic ones. Fig. 4 also shows that for high conversion levels and low particle sizes (0.04 mm and 0.2 mm), the char reactivity shows unexpected trends. For instance, considering steam gasification, the reactivity of char004 becomes very similar to that of char02 at $X = 0.5$ but then dropped below it. In the same way, considering CO₂ gasification, char004, char02 and char035 exhibited the same reactivity

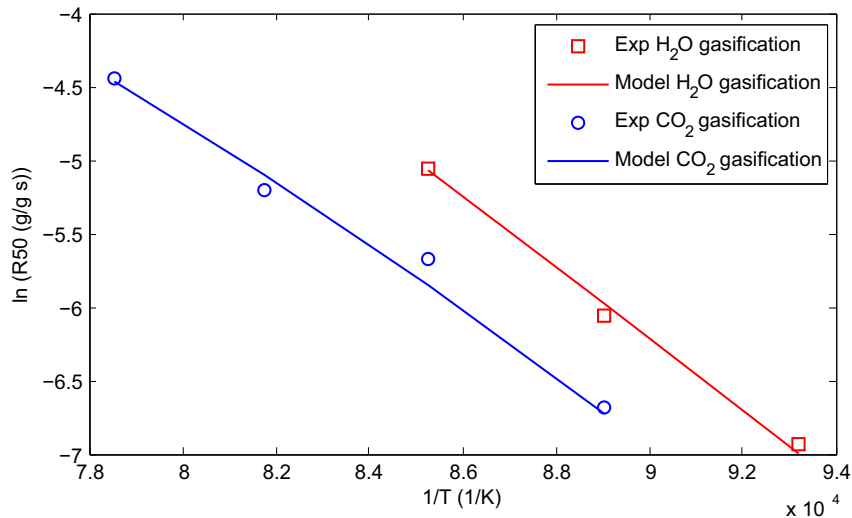


Fig. 8. Arrhenius plots for H₂O and CO₂ gasification: experimental data and models.

Table 6
Kinetic parameters.

	E (kJ·mol ⁻¹)	A (kg·s ⁻¹ ·m ⁻² ·atm ⁻¹)
H ₂ O gasification	207.95	4.16 10 ³
CO ₂ gasification	202.19	1.56 10 ³

at $X = 0.7$. The reactivity of char004 and char02 was equal for higher conversion levels while that of char02 was lower.

Observations derived from the present study as well as from previous ones on char gasification showed that at high conversion levels there are many phenomena that we do not really master or understand. We observed, as well as other authors, many unexpected reactivity behaviours beyond 70% of conversion that change with the type of reacting gas, particle size, pyrolysis atmosphere or temperature. We think that there are several factors (retention/volatilisation of minerals, fragmentation, shrinking) whose effects are different according to particle size, temperature and reacting gas, and which are accentuated at higher conversion levels [2,5,20,22,39,40]. As the experimental repeatability is good, and as it can be deduced from the error bars, we think that these results are related to the gasification mechanism rather than to repeatability issues. Our research is ongoing to understand what phenomena are involved at the final stages of gasification.

The normalized $R(50)$ for the different particle sizes with respect to the $R(50)$ of char004 is illustrated in Fig. 5. A semi log scale is adopted for a better representation. For the two gasification reactions, increasing the char particle beyond 0.04 mm induced nearly the same relative reactivity decrease. This result indicates the equivalence of the reaction diffusion competition for the two gasification reactions. This will be discussed in more detail in the next paragraphs.

Fig. 6 shows the experimental $R(50)$ as well as the Thiele model predictions for H₂O (a) and CO₂ (b) char gasification at 900 °C. As explained above this first step allows determining the best average pore diameter to fit with experimental results. For both H₂O and CO₂ gasification, the pore size for which we obtain the best fit is in the macropore size

range. For H₂O gasification, we found that the best fit is given for a very high pore diameter (a value that has no physical meaning), but when plotting the sum of squared residuals between the experimental data and model prediction as a function of the pore diameter, we observed that this error is constant for pore sizes higher than 1 μm. As shown in Fig. 6 fixing the pore diameter to 1 μm or 5 μm gives quite satisfactory results. In the case of H₂O gasification the pore size would be higher than 1 μm. For CO₂ gasification, the best fit was obtained for a pore size of 1.5 μm. Similarly, when plotting the sum of squared residuals between the experimental data and model prediction as a function of the pore diameter, we obtained a minimum around this value but the experimental data still well represented pore sizes in the range of 0.5 to 5 μm. This range of pores would be most influencing during CO₂ gasification. These results mean that the gasification reactions are mainly occurring in macropores. Some authors think that mesopores and macropores are better indicators of the char reactivity. The contribution of micropores to the active surface area is thought to be negligible compared to that of macropores and large mesopores [26]. To assess if the model captures the experimental data for other pore sizes, we fixed the pore size at some specific values: 1 nm (micropores), 30 nm (mesopores) and 1000 nm (macropores) and searched for k_{900} that allows the best fit to the experimental results. As shown in Fig. 6, neither pore size representative of micropores nor one representative of mesopores allows to capture the experimental $R(50)$. It can also be seen that for the char004, both gasification reactions are performed in the chemical regime. The experimental $R50$ points for the char004 are located in the plateau given by the model so that further reducing the char particle size will not modify the char reactivity.

Diffusional limitations increase with increasing particle size. To illustrate the extent of the diffusional limitations, we present in Fig. 7, the evolution of the effectiveness factor with char particle size for H₂O and CO₂ gasification at 900 °C. The similarity in the evolution of η with the particle size means that the reaction diffusion competition is similar for both gasification reactions. However, H₂O is found to react and diffuse faster than the CO₂ molecule which has lower chemical reactivity and

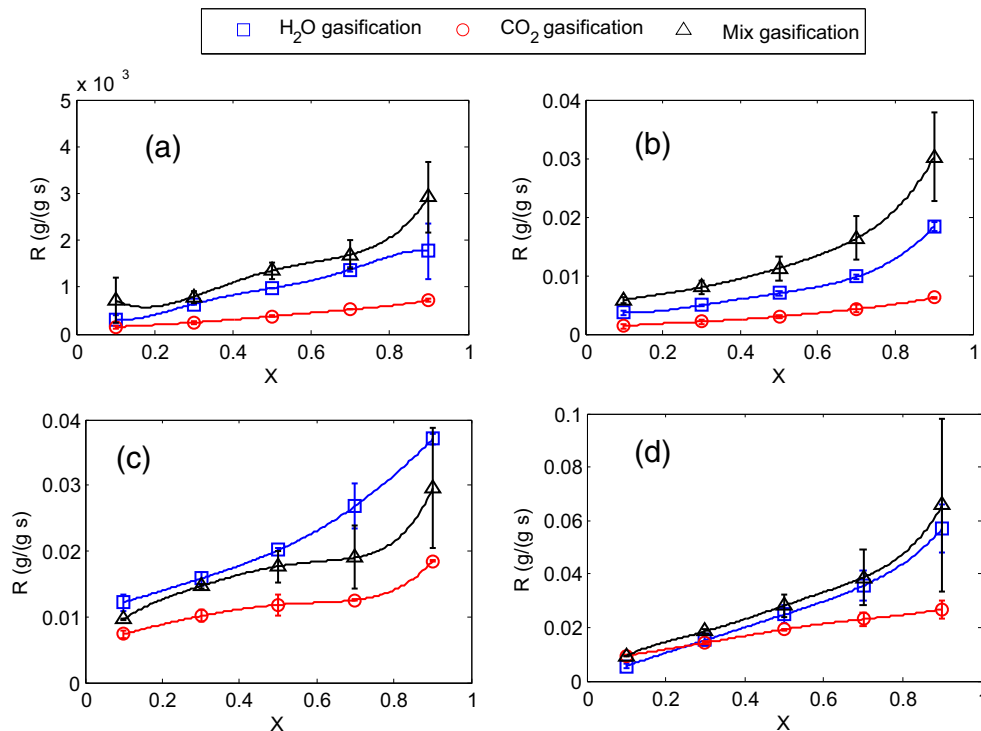


Fig. 9. Char02 gasification reactivity in 20% H₂O, 20% CO₂ and 20% H₂O + 20% CO₂ at 800 °C (a), 900 °C (b), 1000 °C (c) and 1100 °C (d).

diffusivity due to its bigger molecular size. The ratio of H₂O and CO₂ reactivities is around 2 while the effective diffusive coefficients are 5.10^{-5} m²/s for H₂O and 3.10^{-5} m²/s for CO₂. It can be seen in this figure that for both reactions increasing the particle size from 0.04 mm to 13 mm induced the reactivity to decrease by more than twenty folds.

The kinetic parameters, namely A and E were determined by fitting the R(50) data for char02 with the Thiele model at various temperatures for the H₂O and CO₂ gasification reactions. Arrhenius plots are shown in Fig. 8 for both reactions. The model fits quite well to the experiments. The values of A and E are given in Table 6. They match well with the values given in Di Blasi's review on lignocellulosic biomass char gasification with CO₂ and H₂O [2]. The activation energies for both reactions are around 200 kJ/mol which is quite close to the findings of [23] who found equivalent values for beech wood char gasification with H₂O and CO₂.

We found that for the 0.2 mm particle size, both gasification reactions would be performed in the chemical regime at 800 °C with η being very close to one. Diffusional limitations become non negligible at 900 °C with an effectiveness factor of around 0.92. At 1000 °C, the effectiveness factor for both reactions is around 0.7 for the 0.2 mm sized char particles.

3.2. Gasification experiments in mixed atmospheres of H₂O and CO₂

3.2.1. Effect of temperature on the mixed atmosphere gasification

The effect of temperature on mixed atmosphere gasification was studied for the char02 sample. Char02 gasification reactivities in single

and mixed atmospheres of H₂O and CO₂ at 800 °C, 900 °C, 1000 °C and 1100 °C are shown in Fig. 9. It can be seen in the figure that the char reactivity towards H₂O is higher than that towards CO₂ at all temperatures, except in the very beginning of the reaction at 1100 °C where the reactivity to CO₂ was a little bit higher. We think that this observation is related to morphological modifications or loss of catalysts occurring at high temperatures. With the reaction unfolding, H₂O reactivity was higher than that of CO₂ reactivity.

Concerning mixed atmosphere gasification, we can observe that the reactivity in the mixed atmosphere of 20% H₂O + 20% CO₂ is higher than the reactivity towards steam at 800 and 900 °C. The sum of the individual reactivities approaches that observed in mixed atmosphere gasification. We may think that at these temperatures the two gases react separately without any kind of inhibition. At these temperatures and for a total partial pressure of reacting molecules of 40mol%, there would be enough active sites for the two gases to react on. At 1000 °C inhibition was observed. The reactivity in the mixed atmosphere is lower than that with steam alone but higher than that obtained under CO₂ atmosphere. At 1100 °C, the char reactivity at the very beginning is similar to that obtained at 1000 °C. At these two temperatures, the reaction kinetics becomes quite fast and there would exist high diffusional limitations. The reacting gases react only on a portion of the active area and the concentration of active sites is therefore reduced. There is consequently a manifestation of competition resulting in a reactivity in mixed atmospheres lower than that of the sum of the individual reactivities. In addition, the competition mechanism may be accentuated by

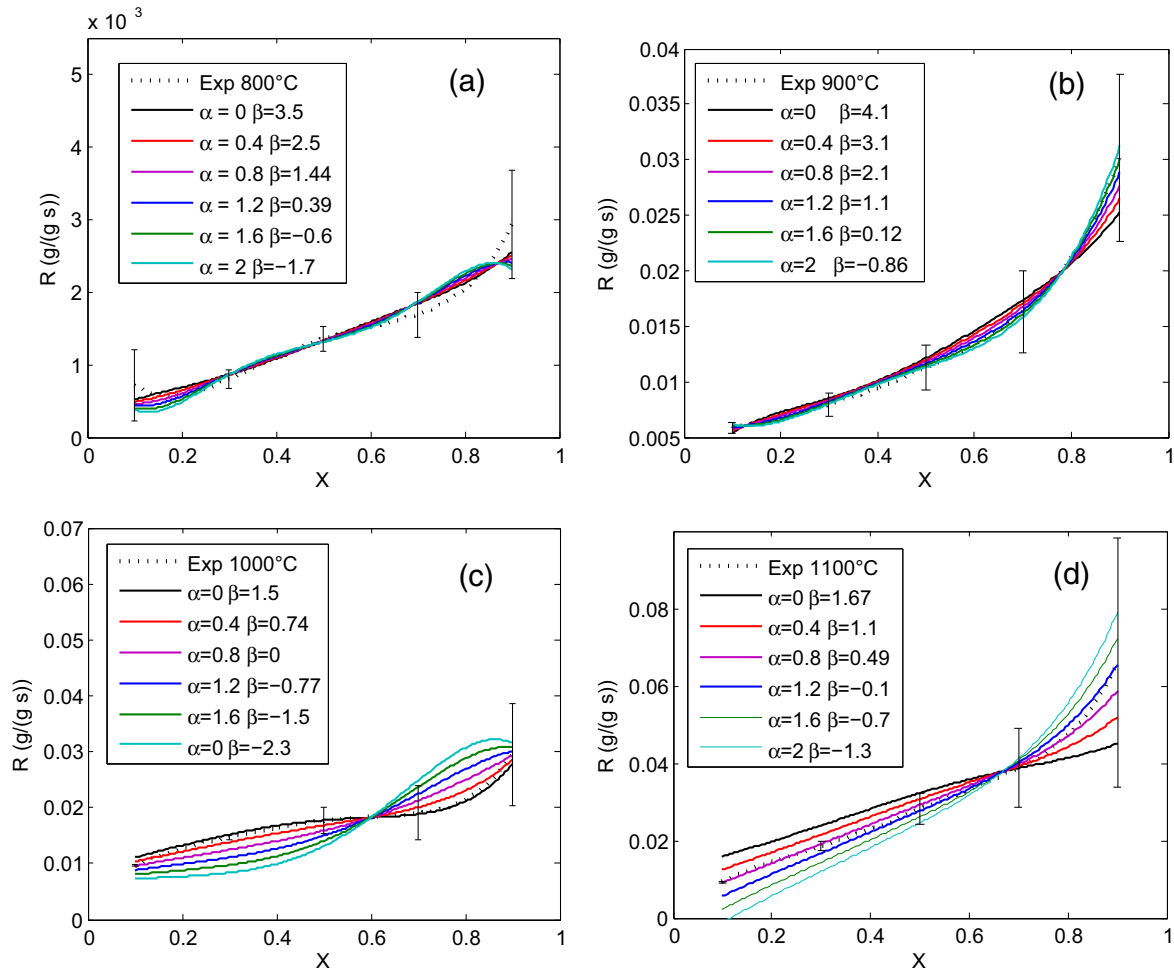


Fig. 10. Modelled mixed atmosphere reactivities for different combinations of α and β and their confrontation to the experimental results at 800 °C (a), 900 °C (b), 1000 °C (c) and 1100 °C (d).

structural modifications at higher temperatures, thermal annealing by an ordering of the carbonaceous matrix and loss of functional groups constituting the active sites [41]. A reduced catalytic effect can be also at the origin of this observation, as catalytic species like *K*, *Ca*, *Mg* or *Na* may volatilize or sinter at high temperature [42]. A high temperature reaction can contribute to an increase in the volatility of catalytic species [43]. The combination of experimental parameters of temperature, active site concentration and reacting gas partial pressure determine the extent of competition or reaction on separate active sites as proposed recently by Roberts et al. [44]. Owing to these results we can conclude that the gasification mechanism varies with the type of char (active site concentration, presence of catalytic species), the temperature (influencing the reaction rate and char properties) and reacting molecule concentration (active site saturation).

The experiments as well as the modelling results on char reactivity on mixed atmospheres are shown in Fig. 10. In the modelling procedure, α and β that ensure the best fit to the experiments are given for the lowest value of the objective function. However, there may be several combinations of α and β that may give satisfactory results. In order to check if the solutions obtained for the different temperatures are unique, we fixed manually, in a second modelling run, the value of α and searched that of β that gives the best fit to the experimental data. α was varied between 0 and 2 by a step of 0.4.

At 800 °C, the gasification reaction is thought to be performed in the chemical regime. The reactivity in the mixed atmosphere is best described by an additive law since $\alpha = \beta = 1$ according to the optimisation procedure. Nevertheless, regardless of the combination of α and β , the modelled reactivity is found in the range of the experimental standard deviation zone. For β to remain positive, α must be in the range of 0 to 1.35 which is quite a wide range to state about the mechanism of mixed atmosphere gasification at 800 °C. Similarly at 900 °C, while α is comprised between 0 and 1.65, all combinations of α and β give satisfactory results. The reactivity curve is in the experimental standard deviation zone.

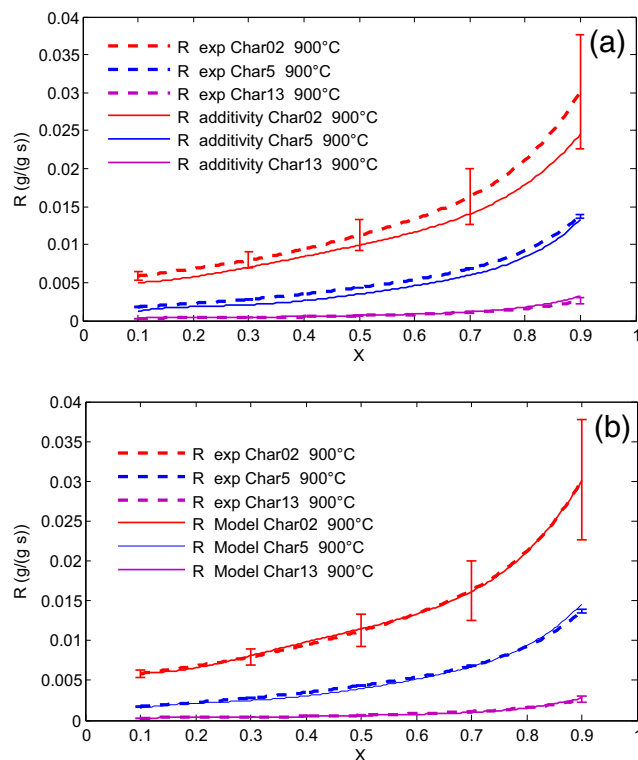


Fig. 11. Experimental char gasification reactivity in 20% H₂O + 20% CO₂ at 900 °C for char02, char5 and char13 and modelling results (a) additivity model and (b) best fit.

At 1000 °C, the situation is a bit different as only values of α below 0.2 and beta between 1.1 and 1.5 allow to correctly describe the experimental reactivity without being out of the standard deviation zone in the conversion level range of 0 to 0.4. At 1100 °C, α is found to be in the range of 0.8–1.1 with β in the range of 0 to 0.48 for the modelled reactivity to be in the standard deviation zone for levels of conversion between 0.1 and 0.3. Beyond $X = 0.3$, all possible combination of α and β give correct predictions. These results indicate that it is not possible to make a statement on the gasification mechanism in mixed atmosphere gasification at 800 °C and 900 °C as wide ranges of α and β are found to reproduce the experimental results. At 1000 °C and 1100 °C, the situation is a bit different as only particular α and β values give correct representations of the reactivity, yet they are limited to the defined conversion ranges out of which it is not possible to define which gas is the most reactive with char. In the literature, as seen in the Introduction section of the present paper, many studies state on the gasification mechanism as it is a passive cooperation from the observation that there is an additive law representing well the reactivity in mixed atmosphere. This statement has to be taken with caution regarding the results of the present studies. What appears to be an additive law may in fact be a more complex mechanism involving competition and synergy effects that result in an additive like mechanism.

3.2.2. Effect of the char particle size on the mixed atmosphere gasification

Fig. 11 shows the char reactivity at a temperature of 900 °C, in a mixed atmosphere of 20% H₂O + 20% CO₂ for the char02, char5 and char13 samples. Decrease in reactivity with size is related to mass transfer limitations as discussed previously. In Fig. 11a, we plotted the experimental reactivities along with an additivity model for which $\alpha = \beta = 1$. As it can be seen in the figure, the additivity model represents quite fairly the char reactivity in mixed atmospheres of H₂O and CO₂. For high diffusional limitations (char13) as well as for quite low ones (char02), the mixed atmosphere char reactivity in 20% H₂O + 20% CO₂ at 900 °C can be fairly considered as the sum of the individual reactivity contributions. The best fit modelling results give values for α and β different from 1. The values of α and β equal respectively 1.61 and 0.1 for char02, 1.58 and 0.1 for char5 and 0.9 and 0.8 for char13. The two gases are likely

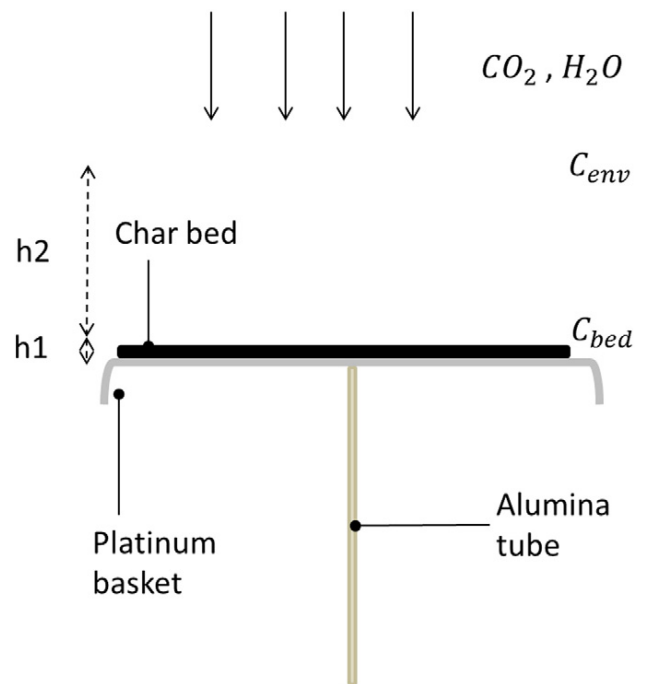


Fig. 12. A schematic representation of the char04 gasification at 900 °C with H₂O or CO₂.

competing for the biggest chars while H₂O seems to have an enhanced activity in the presence of CO₂ for the char02 and char5 samples. However, there exist a wide range of α/β combinations that ensure a good representation of the experimental results, so that we cannot state the contribution of each reaction to the char gasification. This modelling approach allows only to calculate the reactivity in the mixed atmosphere but not to understand the gasification mechanism. Another approach is needed to go deeper into this issue.

4. Conclusion

The objective of the present work was to evaluate the extent of diffusional limitations when varying the temperature and char particle size and also to shed light on the influence of temperature and char particle size on the multi component gasification reaction with CO₂ and H₂O.

Adopting an effectiveness factor approach, we quantified the extent of the internal diffusional limitations in a large char particle size ranging

from 0.04 mm to 13 mm for both H₂O and CO₂ gasification reactions. We found a similar effectiveness factor evolution with particle size for both reactions. The diffusion reaction competition for both gasification reactions was nearly the same for both molecules. However, H₂O was found to have an almost twice higher reactivity and diffusivity than CO₂ explaining the equivalence of the diffusion reaction competition. At 900 °C, the char gasification H₂O or CO₂ would be performed in the chemical regime for char particles of 0.04 mm and below.

In the second part, we assessed the effect of temperature and particle size on mixed atmosphere gasification. The char02 reactivity in the mixed atmosphere of H₂O and CO₂ was nearly equal to the sum of the individual reactivity at 800 °C, a little bit higher at 900 °C and lower than that at 1000 °C and 1100 °C for 0.2 mm sized char particles. High diffusional limitations at 1000 and 1100 °C caused the gasification reaction mechanism to shift from reaction on separate active sites to competition between the two gases to access the char active sites.

Despite the reactivity in mixed atmosphere being well represented by a linear combination of the two individual reactivities, it is not

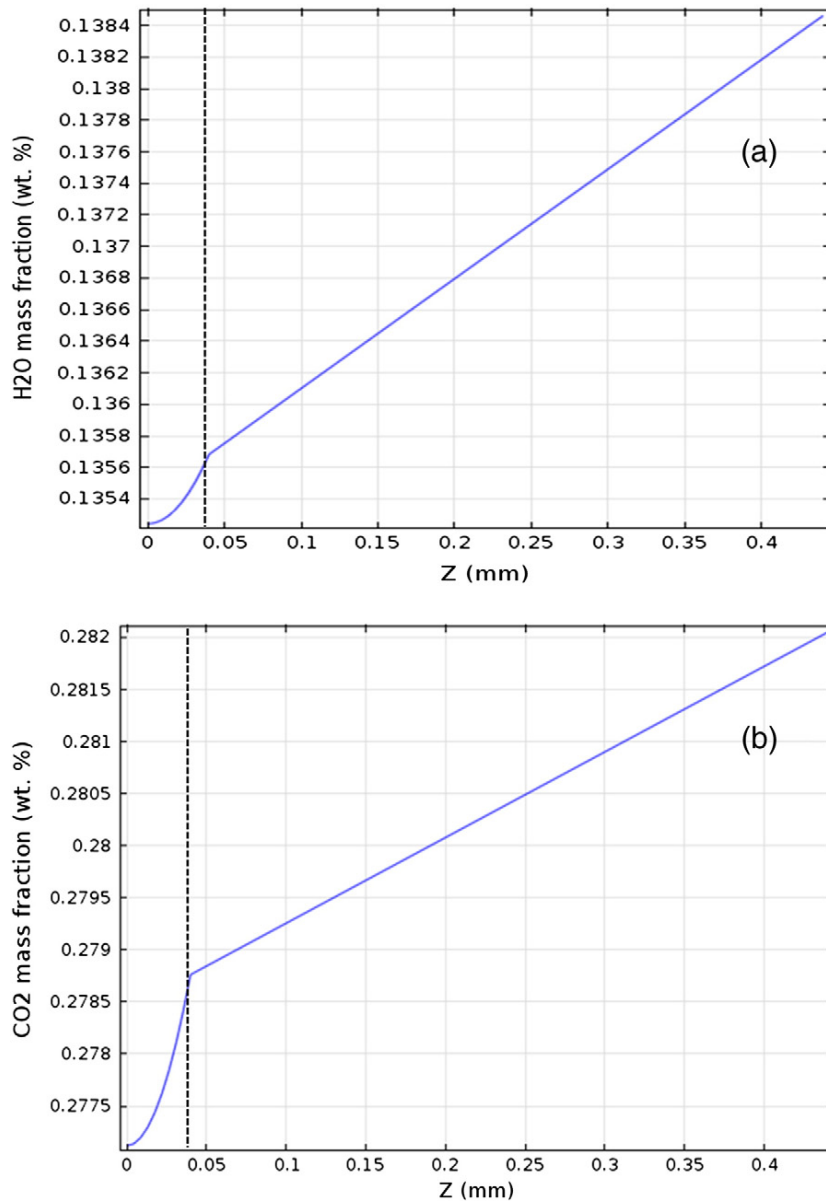


Fig. 13. H₂O (a) and CO₂ (b) mass fractions in the surrounding and in the char bed. The dashed black line represents the interface between the char bed surface and the surroundings.

possible to state on the gasification mechanism due to the wide range of α and β combinations that allow to reproduce correctly the char reactivity, especially at 800 °C and 900 °C. Similar conclusions were drawn when varying the particle size as it was not possible to determine the gasification mechanism due to various linear coefficient combinations allowing to correctly model the char reactivity.

To the best of the authors' knowledge, these results on biomass char gasification in complex atmospheres are quite new in the literature. Further investigations are needed, especially concerning the char property evolution along the gasification reactions in H₂O, CO₂ and in CO₂ + H₂O in order to understand the reaction mechanisms. This issue will be tackled in future works.

Acknowledgements

The authors acknowledge the national research agency ANR France (ANR 10 BIOE 0002) for its financial support in the RECO2 project. They also wish to express their appreciation for Bernard Auduc for his technical support.

Appendix A

To check the accuracy of the thermogravimetric data obtained at 900 °C, so that the reaction rate is effectively determined for a reactant concentration of 20% at the char bed surface, we considered a monodimensional diffusion model involving the external diffusion of the reactant gas (H₂O or CO₂) from the environment where the molar concentration is $C_{env} = 20\%$ to the char bed where the concentration is C_{bed} , and a diffusion within the char bed with a volumetric reaction term (source term) corresponding to the carbon consumption. The study was applied to the case of the 0.04 mm char particles for which the reaction rate is the highest compared to the other bigger particles. The source term is determined from the experimental reactivity obtained at $X = 0.5$. The external diffusion height ($h_2 = 0.4$ mm) is fixed to 10 times that of the internal diffusion inside the char bed ($h_1 = 0.04$ mm).

A schematic representation of the gasification reaction in is shown in Fig. 12.

Fick's second law in a steady state regime gives:

$$\nabla J_i = R_i \quad (20)$$

The suffix "i" designates the gas species involved in the gasification reaction (CO₂, CO and N₂ in the Boudouard reaction, and H₂O, CO, H₂ and N₂ in the steam gasification reaction).

J_i (kg/m²·s) is the diffusive flux calculated by Fick's law:

$$J_i = \rho D_i \nabla \omega_i \quad (21)$$

where:

- ρ : the total gas density (kg/m³)
- D_i : molecular diffusion coefficient (m²/s). The effective diffusion coefficient in the char bed is corrected by the ratio $\frac{\rho}{\rho_0}$.
- ω_i : gas specie "i" mass fraction

R_i (kg/m³·s) is the source term determined from the experimental carbon consumption in the char bed at $X = 0.5$. Stoichiometric considerations allow calculating the source term for each gas species considering the two chemical reactions of Boudouard and steam gasification.



The modelling results are shown in Fig. 13. It can be seen in this figure that the gas concentration at the bed surface is very close to that in

the surroundings. A quite small decrease is found, and thus external diffusional limitations can be assumed to be negligible.

References

- [1] P. Basu, Biomass Gasification and Pyrolysis: Practical Design and Theory, Elsevier, 2010.
- [2] C. Di Blasi, Combustion and gasification rates of lignocellulosic chars, Prog. Energy Combust. Sci. 35 (2009) 121–140 (Apr.).
- [3] M.J. Gronewald, V. S. W.P.M., Gasification of char particles with CO₂ and H₂O, Chem. Eng. Sci. 35 (1980) 307–313.
- [4] M. Barrio, Experimental Investigation of Small-scale Gasification of Biomass (PhD Thesis) The Norwegian University of Science and Technology, 2002.
- [5] J.P. Tagutchu, Gazéification du charbon de plaquettes forestières: particule isolée et lit fixe continu (PhD thesis) Université de perpignan, 2008.
- [6] D. Roberts, D. Harris, Char gasification in mixtures of CO₂ and H₂O: competition and inhibition, Fuel 86 (2007) 2672–2678 (Dec.).
- [7] H.C. Butterman, M.J. Castaldi, Influence of CO₂ injection on biomass gasification, Society (2007) 8875–8886.
- [8] H.C. Butterman, M.J. Castaldi, CO₂ as a carbon neutral fuel source via enhanced biomass gasification, Environ. Sci. Technol. 43 (2009) 9030–9037 (Dec.).
- [9] S. Nilsson, A. Gómez-Barea, P. Ollero, Gasification of char from dried sewage sludge in fluidized bed: reaction rate in mixtures of CO₂ and H₂O, Fuel 105 (2013) 764–768 (Mar.).
- [10] S. Nilsson, A. Gómez-Barea, D. Fuentes-Cano, M. Campoy, Gasification kinetics of char from olive tree pruning in fluidized bed, Fuel 125 (2014) 192–199 (June).
- [11] C. Guizani, F. Escudero Sanz, S. Salvador, The gasification reactivity of high-heating-rate chars in single and mixed atmospheres of H₂O and CO₂, Fuel 108 (2013) 812–823 (June).
- [12] T. Lilledahl, K. Sjöström, Modelling of char–gas reaction kinetics, Fuel 76 (1) (1997) 29–37.
- [13] R.C. Everson, H.W. Neomagus, H. Kasaini, D. Njapha, Reaction kinetics of pulverized coal-chars derived from inertinite-rich coal discards: gasification with carbon dioxide and steam, Fuel 85 (2006) 1076–1082 (May).
- [14] Z. Huang, J. Zhang, Y. Zhao, H. Zhang, G. Yue, T. Suda, M. Narukawa, Kinetic studies of char gasification by steam and CO₂ in the presence of H₂ and CO, Fuel Process. Technol. 91 (2010) 843–847 (Aug.).
- [15] H.-L. Tay, S. Kajitani, S. Zhang, C.-Z. Li, Effects of gasifying agent on the evolution of char structure during the gasification of Victorian brown coal, Fuel 103 (2013) 22–28. <http://dx.doi.org/10.1016/j.fuel.2011.02.044> (ISSN 0016-2361).
- [16] C. Chen, J. Wang, W. Liu, S. Zhang, J. Yin, G. Luo, H. Yao, Effect of pyrolysis conditions on the char gasification with mixtures of CO₂ and H₂O, Proc. Combust. Inst. 34 (2013) 2453–2460 (Jan.).
- [17] S. Umamoto, S. Kajitani, S. Hara, Modeling of coal char gasification in coexistence of CO₂ and H₂O considering sharing of active sites, Fuel 103 (2013) 14–21 (Jan.).
- [18] Y. Bai, Y. Wang, S. Zhu, L. Yan, F. Li, K. Xie, Synergistic effect between CO₂ and H₂O on reactivity during coal chars gasification, Fuel (2014) 1–7 (Feb.).
- [19] A. Gómez-Barea, P. Ollero, C. Fernández-Baco, Diffusional effects in CO₂ gasification experiments with single biomass char particles. 1. Experimental investigation, Energy Fuel 20 (2006) 2202–2210 (Sept.).
- [20] F. Mermoud, F. Golfier, S. Salvador, L. Vandesteene, J. Dirion, Experimental and numerical study of steam gasification of a single charcoal particle, Combust. Flame 145 (2006) 59–79 (Apr.).
- [21] F. Mermoud, Gazéification de charbon de bois à la vapeur d'eau: de la particule isolée au lit fixe continu (PhD thesis) INPT Toulouse 2006.
- [22] L. Van de steene, J. Tagutchou, F. Escudero Sanz, S. Salvador, Gasification of woodchip particles: experimental and numerical study of charH₂O, charCO₂, and charO₂ reactions, Chem. Eng. Sci. 66 (2011) 4499–4509 (Oct.).
- [23] W. Klose, M. Wolki, On the intrinsic reaction rate of biomass char gasification with carbon dioxide and steam, Fuel 84 (2005) 885–892 (May).
- [24] T. Pattanotai, H. Watanabe, K. Okazaki, Experimental investigation of intraparticle secondary reactions of tar during wood pyrolysis, Fuel 104 (2013) 468–475 (Feb.).
- [25] U. Henriksen, C. Hindsgaul, B.R. Qvale, F. Jjellerup, A.D. Jensen, Investigation of the anisotropic behavior of wood char particles during gasification, Energy Fuel 20 (2006) 2233–2238 (Sept.).
- [26] F. Mermoud, S. Salvador, L. Vandesteene, F. Golfier, Influence of the pyrolysis heating rate on the steam gasification rate of large wood char particles, Fuel 85 (2006) 1473–1482 (July).
- [27] A. Sadezky, H. Muckenhuber, H. Grothe, R. Niessner, U. Pöschl, Raman microspectroscopy of soot and related carbonaceous materials: spectral analysis and structural information, Carbon 43 (2005) 1731–1742 (July).
- [28] P. Ollero, A. Serrera, R. Arjona, S. Alcantarilla, The CO₂ gasification kinetics of olive residue, Biomass Bioenergy 24 (2003) 151–161 (Feb.).
- [29] M. Barrio, B. Gøbel, H. Risnes, U. Henriksen, J.E. Hustad, N.K. Allé, D.-K. Lyngby, Steam gasification of wood char and the effect of hydrogen inhibition on the chemical kinetics, in: A.V. Bridgwater (Ed.) Progress in Thermochemical Biomass Conversion, 2001, pp. 32–46.
- [30] F.A. Tanjung, Gasification of single wood particles in CO₂, Fuel 67 (1988) 666–672.
- [31] K. Umeki, S.-A. Roh, T.-J. Min, T. Namioka, K. Yoshikawa, A simple expression for the apparent reaction rate of large wood char gasification with steam, Bioresour. Technol. 101 (2010) 4187–4192 (June).
- [32] A. Gómez-Barea, Modelling of Diffusional Effects During Gasification of Biomass Char Particles in Fluidised-bed (PhD Thesis) University of Seville, 2006.
- [33] W. Huo, Z. Zhou, F. Wang, Y. Wang, G. Yu, Experimental study of pore diffusion effect on char gasification with CO₂ and steam, Fuel 131 (2014) 59–65 (Sept.).

- [34] T. Mani, N. Mahinpey, P. Murugan, Reaction kinetics and mass transfer studies of biomass char gasification with CO₂, *Chem. Eng. Sci.* 66 (2011) 36–41 (Jan.).
- [35] E.W. Thiele, Relation between catalytic activity and size of particle, *Ind. Eng. Chem.* 31 (7) (1939) 916–920.
- [36] A. Bliiek, J. Lont, W. van Swaaij, Gasification of coal-derived chars in synthesis gas mixtures under intraparticle mass-transfer-controlled conditions, *Chem. Eng. Sci.* 41 (1986) 1895–1909 (Jan.).
- [37] A. Gomezbarea, P. Ollero, A. Villanueva, Diffusional effects in CO₂ gasification experiments with single biomass char particles. 2. Theoretical predictions, *Energy Fuel* 2 (2006) 2211–2222.
- [38] S. Nilsson, A. Gómez-Barea, D.F. Cano, Gasification reactivity of char from dried sewage sludge in a fluidized bed, *Fuel* 92 (2012) 346–353 (Feb.).
- [39] S. Valin, M. Grateau, S. Thiery, G. Gauthier, F. Defoort, T. Melkior, Influence of atmosphere (N₂/CO₂/H₂O) on wood centimetre-scale particle devolatilisation at 800 °C, *Fuel* 139 (2015) 584–593 (Jan.).
- [40] C. Hognon, C. Dupont, M. Grateau, F. Delrue, Comparison of Steam Gasification Reactivity of Algal and Lignocellulosic Biomass: Influence of Inorganic Elements, *Bioresource Technology*, 2014. (May).
- [41] B. Feng, Structural ordering of coal char during heat treatment and its impact on reactivity, *Carbon* 40 (2002) 481–496 (Apr.).
- [42] A. Zolin, A. Jensen, P.A. Jensen, F. Frandsen, K. Dam-Johansen, The influence of inorganic materials on the thermal deactivation of fuel chars, *Energy Fuel* 15 (2001) 1110–1122 (Sept.).
- [43] D.M. Keown, G. Favas, J.-I. Hayashi, C.-Z. Li, Volatilisation of alkali and alkaline earth metallic species during the pyrolysis of biomass: differences between sugar cane bagasse and cane trash, *Bioresour. Technol.* 96 (2005) 1570–1577 (Sept.).
- [44] D.G. Roberts, D.J. Harris, Char gasification kinetics in mixtures of CO₂ and H₂O: the role of partial pressure in determining the extent of competitive inhibition, *Energy Fuel* 28 (2014) 7643–7648.